Journal of the Australian Ceramic Society
https://doi.org/10.1007/s41779-018-0201-8

RESEARCH

Synthesis and characterization of lignite fly ash ceramic substrates coated with TiO_2 slurry, and evaluation in environmental applications

E. Katsika[1] · A. Moutsatsou[1] · V. Karayannis[2] · M. Volioti[1] · D. Tsoukleris[3]

Received: 23 October 2017 / Revised: 13 April 2018 / Accepted: 1 May 2018

Abstract

The novel valorization of lignite combustion fly ashes in the development of ceramic substrates modified with TiO_2 photocatalyst, with environmental benefits, was investigated. Disc-shaped compacts from fly ashes (either calcareous or siliceous) were sintered (1000 °C, 2 h), then coated with TiO_2 slurry, and further thermally treated (400 and 500 °C, 1 h) to acquire TiO_2 consistency onto the ceramic substrate. The ceramic microstructures were examined by XRD and SEM-EDAX. Their photocatalytic activity was examined in aqueous solutions of two organic dyes, methylene blue and methyl orange using visible and UV irradiation, with encouraging results. A synergistic effect between ash ceramic substrates and TiO_2 enhances the properties of the final activated product. Pores occurring on the non-activated ash surface are to some extent covered by TiO_2. As a result, the photocatalytic activity, rather than simple dye adsorption onto the surface of the coated substrates, is promoted leading to efficient dye decolorization. Higher dye removal is achieved in the case of methylene blue under cool daylight compared to methyl orange under UV (blacklight and blacklight blue). A major advantage of the process is the immobilization of TiO_2 onto a cheap porous substrate, which can provide an alternative for the photocatalytic treatment of industrial effluents.

Keywords Lignite fly ash · Ceramic, substrate · TiO_2 · Coating · Photocatalytic activity

Introduction

The valorization of industrial residues as secondary resources in the elaboration of value-added materials is important for environmental protection, resources conservation, and cost reduction. Moreover, current advances in environmental legislation encourage manufacturers to optimize industrial by-products' management and utilization. In particular, the valorization of fly ash (FA) produced in massive quantities from coal/lignite combustion for power generation is nowadays of increasing importance. The recycling of FA can be a good alternative solution to disposal. The global average utilization rate of FA is estimated to be nearly 25% of the production. Advances in the development of cement, zeolite, water glass, composite concrete, sintered ceramics, catalysts, and filler in polymers as well as other lightweight construction materials, establish that further beneficial utilization of industrial by-products is not only possible but also energy and cost efficient [1–5].

More than 8 million tons of ashes are annually produced from lignite combustion in Greek Power Stations. Fly ashes of both types, calcareous and siliceous, are generated in lignite-fed power stations situated in Northern and Southern Greece respectively. Indeed, approx. 80% of this amount comes from Northern Greece (Region of Western Macedonia) where the main lignite deposits are located. Only a small amount of Greek FA is currently used, while most of the overall ash output is directly discharged into ponds and landfills. In previous studies, lignite ashes have been tested by the authors for the production of standard ceramics by conventional and microwave furnace sintering [6, 7].

✉ V. Karayannis
vkarayan62@gmail.com

[1] Laboratory of Inorganic and Analytical Chemistry, School of Chemical Engineering, National Technical University of Athens (NTUA), Zografou Campus, 15773 Athens, Greece

[2] Laboratory of Waste Management Technologies, Department of Environmental Engineering, Western Macedonia University of Applied Sciences, 50100 Kozani, Greece

[3] Laboratory of General Chemistry, School of Chemical Engineering, National Technical University of Athens (NTUA), Zografou Campus, 15773 Athens, Greece

Published online: 11 May 2018

The chemical, mineralogical, and morphological characteristics of these by-products promote their application in the field of ceramics substrates development. Such substrates can possibly be used for the elaboration of heterogeneous catalysts due to their components [8]. On the other side, TiO_2 is the most appropriate and the most commonly used semiconductor in heterogeneous photocatalytic oxidation, with significant advantages and excellent physicochemical and photocatalytic properties in comparison to the other semiconductors [9–11]. TiO_2 catalyst appears in three crystalline phases in nature, anatase (tetragonal), rutile (tetragonal), and brookite (orthorhombic). Rutile is the most stable form, whereas anatase and brookite phases are metastable and can be transformed to rutile phase when heated under high temperature (~ 750 °C). Anatase and rutile are most often reported as photocatalysts, and recent research results demonstrated that a mixed form of rutile and anatase displayed enhanced photocatalytic ability, since the transfer of electrons from anatase to a lower-energy rutile electron-trapping site in mixed-phase could reduce the combination rate of charge carriers in anatase and effectively create catalytic "hot spots" [12]. So far, blast furnace ash as well as agricultural and ash by-products have been studied as substrates for their photocatalytic ability. Techniques that have been investigated for depositing TiO_2 onto the surface of these materials are the co-grinding at high temperatures [13], the sol-gel method [14, 15], precipitation, thermal spraying, deposition [16], pulsed power, and others [17].

The present research focuses on the innovative surface activation of ceramic substrates made of either siliceous or high-calcium lignite combustion ash by coating them with TiO_2 slurry. The microstructures obtained are studied in relation to TiO_2 coating, drying and thermal treatment conditions. Apart from eliminating the obstacles encountered with the use of the catalyst in the form of particle dispersions and suspensions (need for solid-liquid separation after treatment, particle aggregation, etc.), another significant advantage of the whole process of photocatalyst immobilization is the potential for photocatalytic degradation of persisting pollutants, and also the remaining capacity for adsorption of hazardous heavy metals, as it was concluded from the experiments. The effect of iron oxide, existing in lignite fly ash as an impurity, on the photocatalytic activity of TiO_2 is also discussed.

Experimental

Materials

Highly calcareous fly ash sample (class-C according to ASTM C 618) was obtained from the electrostatic precipitators of the Agios Dimitrios lignite power plant (FAAD) situated in Northern Greece (Region of Western Macedonia). Megalopolis (Sothern Greece) fly ash (FAM) is strongly siliceous, as almost half of it consists of SiO_2 and lesser amounts of Ca-bearing species. Therefore, FAM is barely a class-C ash.

Both types of ashes were evaluated in terms of their chemical composition, by means of X-ray fluorescence (XRF, X-Lab 2000 EDAX), loss on Ignition (ASTM D7348), pH (ISO 6588), and free CaO (CaOf-ASTM C151). Mineralogical analysis was performed by X-ray Diffraction (Siemens D-500), while the particle size distribution of the ashes was determined using Malvern MasterSizer-S by applying the wet dispersion method in water.

The chemical content, the physicochemical characteristics and the mineralogical analysis for these ashes are given in Tables 1 and 2 and Fig. 1 respectively.

The main crystalline phases of FAAD are gypsum ($CaSO_4.2H_20$), quartz (SiO_2), lime (CaO), calcite ($CaCO_3$), and a-hematite (Fe_2O_3). On the other hand, the main mineralogical phases of FAM are quartz (SiO_2), silicon oxide (SiO_2), periclase (MgO), and iron oxide (Fe_2O_3).

Ceramic substrate preparation

Disc-shaped green compacts (13 mm diameter and 3 mm width) from both FAAD and FAM were prepared by uniaxially cold pressing in a stainless steel die using a hydraulic press (Specac, 15011), and then consolidated using sintering procedure in a laboratory chamber programmable furnace (Thermoconcept, KL06/13). A temperature lower than the vitrification point of the ashes was selected as a peak sintering temperature (1000 °C) with 2-h soaking time. Finally, the sintered specimens were gradually cooled to ambient temperature into the furnace. Then the specimen surfaces were coated with TiO_2 slurry (8% TiO_2, 89.9% water and 2.1% disruptive factor), and subsequently exposed (i) to drying in air for 1 day or (ii) heating at 300–500–700 °C for 1 h to acquire the TiO_2 consistency on the ceramic substrate.

Table 1 Chemical analysis of FAAD and FAM

(%)	SiO_2	Al_2O_3	Fe_2O_3	CaO	MgO	SO_3	Na_2O	K_2O	Loi	
FAAD	30.16	14.93	5.10	34.99	2.69	6.28	1.01	0.40	3.95	*CaOf, 10.87%
FAM	49.54	19.25	8.44	11.82	2.27	3.91	0.53	1.81	2.10	*CaOf, 5.95%

Table 2 Physicochemical characteristics of ashes

	pH	Particle size distribution (μm)		Specific weight (g/cm^3)
		D (v, 0.5)	D (v, 0.9)	
FAAD	12.5	30.92	98.28	2.67
FAM	11.8	98.92	199.87	2.62

The obtained microstructures were thoroughly examined by XRD and SEM-EDAX (Jeol, JSM-6400). Also, the difference of the ceramics substrate microstructures was examined after the second heating for the surface consistency. Shrinkage of the samples was calculated as the volume change (%) upon sintering. Apparent density was measured according to the Archimedes principle by means of a specific apparatus (Shimadzu, SMK401-AUW220V). Vickers microhardness was measured with a load of 50 g and a dwell time of 15 s (Wilson Instruments, Mode 402MVD, KnoopVickers Tester). In order to enable reliable comparisons, mean microhardness values over five valid indentations per specimen were calculated. Moreover, the surface roughness of the coated substrates, expressed as arithmetic mean height (Sa), was determined (Bruker, Nano Surfaces Division, CountourGT, Vision 64 Software). Furthermore, the potential of the substrates developed for adsorption of heavy metals, namely, Cu, Pb, Cd, and Zn, was examined.

Photocatalytic activity

The photocatalytic activity of the materials produced was evaluated in the decolorization of two organic dyes (potential pollutants), as a function of time, under visible (daylight) or UV (UV-A) irradiation. The dye used in the experiments under visible irradiation was methylene blue (MB), a cationic dye with molecular formula $C_{16}H_{18}ClN_3S$, while the dye used under UV irradiation was methyl orange (MO), an anionic dye with molecular formula $C_{14}H_{14}N_3NaO_3S$. The selection of MB and MO was made because they are commonly used as standard pollutant compounds in many studies, and their absorption is easy to detect through spectrophotometry measurements. Furthermore, organic dyes are important and common effluents of textile industry [18–20].

Synthetic aqueous solutions of MB and MO with initial concentrations of 0.4×10^{-5} and 1.7×10^{-5} M respectively were prepared, by dissolving dye powder (Fluka and Merck respectively) in distilled water. The solutions were saturated in oxygen by bubbling O_2 in the solution for 1.5 h prior to use. The photocatalytic process was carried out in round-bottom photocatalytic Pyrex glass cells that are transparent to wavelengths above 320 nm. The activated disc-shaped substrates were cut in surface areas of about 1 cm^2 and inserted in the photocatalytic cell with 5 ml of the dye solution.

The laboratory system used for the irradiation of the cells with the samples was equipped with four parallel OSRAM L15W/865 LUMILUX Cool Daylight tubes for the

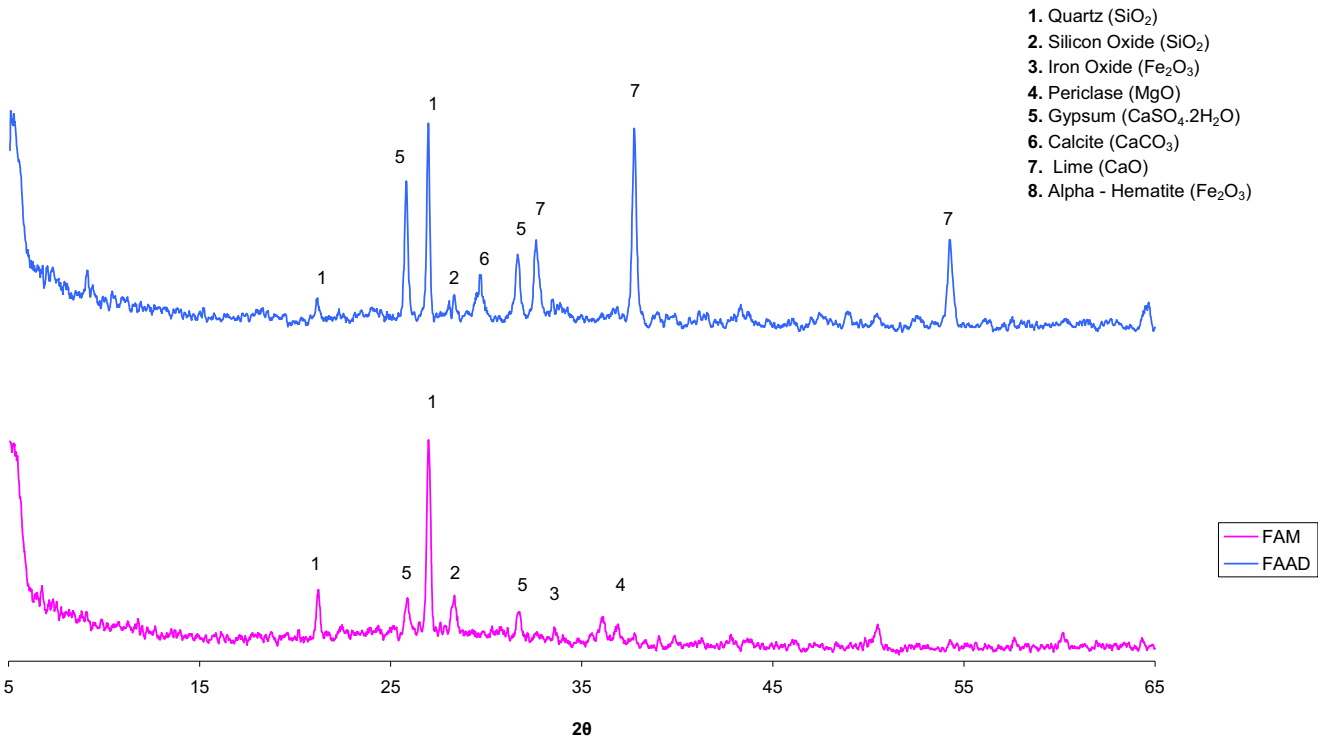

Fig. 1 Mineralogical analysis of FAAD and FAM

experiments under visible light. For UV irradiation, two experiment series were carried out, using either SYLVANIA blacklight 368 F15W/T8/BL368 tubes with maximum emission at 368 nm, either SYLVANIA blacklight blue F15W/BLB-T8 tubes with maximum emission at 350 nm. The selection of light source for each type of pollutant was made taking under consideration the optical spectrum of the two dyes and the possible presence of absorption bands near the irradiation wavelength of the lamps, so as to avoid the occurrence of side reactions.

All photocatalytic experiments were performed under continuous magnetic stirring, while pH and temperature values of the solutions were maintained constant. Before adding the catalyst, pH of MB και MO aqueous solutions was 6.5 and 8.2 respectively, but upon addition of the alkaline lignite ash, pH increased. After pH optimization trials, the reaction was found to be effective when the solution was regulated at pH 5.4–5.5.

The decomposition of the dye pollutants as a function of time and the rate of decolorization were spectrophotometrically determined (UV-VIS Spectrophotometer HITACHI U-2001) by recording the absorption spectra of samples taken out at specific time intervals and measuring the change in intensity of the characteristic peak at the maximum absorption wavelength of the dyes ($\lambda_{max,MB}$ = 664.0 nm, $\lambda_{max,MO}$ = 463.0 nm) [18, 21, 22]. Then, the adsorption and photocatalytic dye decomposition efficiency was determined using the following equation:

$$\text{Efficiency}\ (\%) = (C_0 - C)100/C_0$$

where C_0 is the initial concentration of dye solution and C is the final concentration after illumination by visible or UV light.

Results and discussion

XRD spectra of the coating of the ceramic substrates under different thermal treatment conditions are presented in Fig. 2. It can be seen that the main mineral phases of all coated surfaces are anatase and rutile. The phase of the small peak detected between rutile and anatase at the calcination temperatures of 500 and 700 °C is quartz (SiO_2).

The mineralogical analysis of the ceramic substrates obtained either from FAAD or FAM fly ash is shown in Fig. 3a, b respectively. For the ceramic substrates made of FAAD, the main phases are anhydrite and quartz. In the green specimen (Fig. 3a (A)), the intensity of the peak associated with lime (CaO) predominates. The ash sintered up to 1000 °C (Fig. 3a (B)) and those further thermally treated after coating (Fig. 3a (C)) exhibit different mineralogical compositions, and

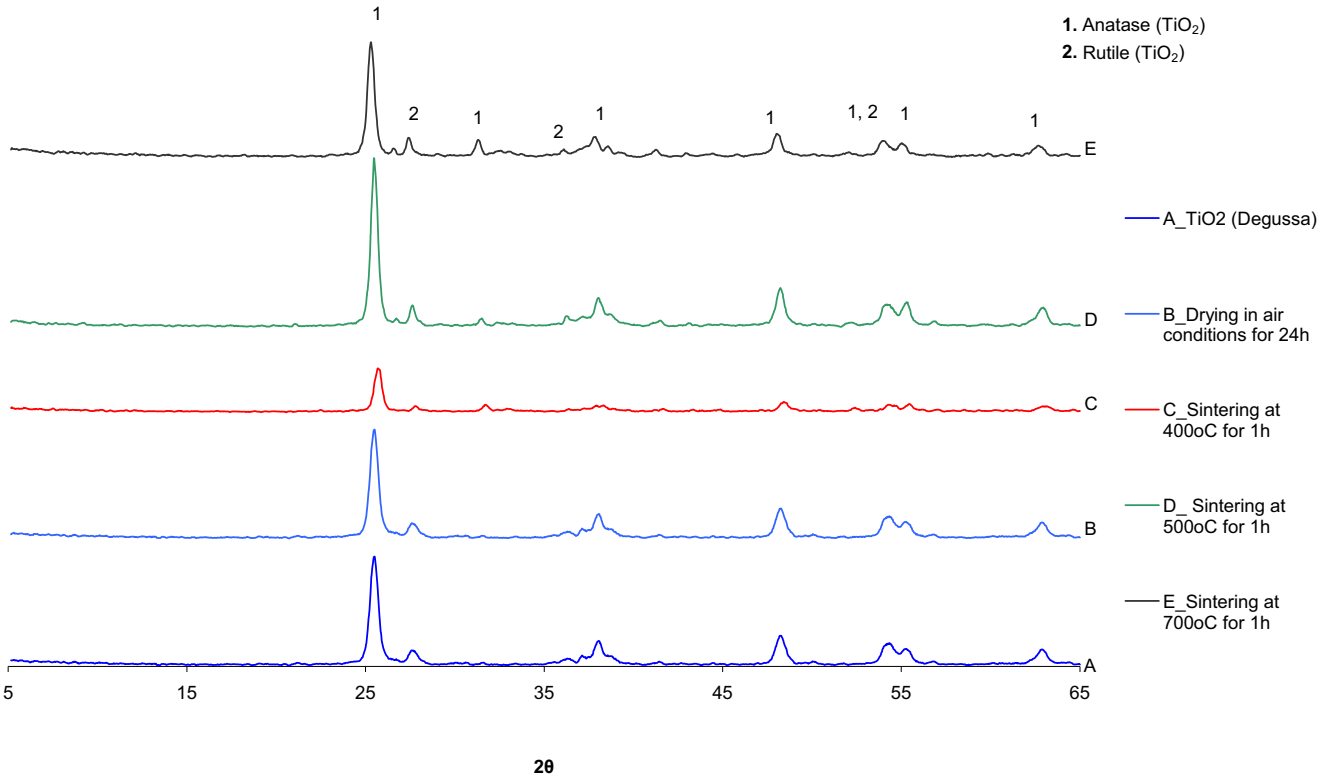

Fig. 2 XRD spectra of the coating of the ceramic substrates (A) TiO_2 (Degussa), (B) dried at air condition (C) sintered at 400 °C for 1 h, (D) sintered at 500 °C for 1 h and (E) sintered at 700 °C for 1 h

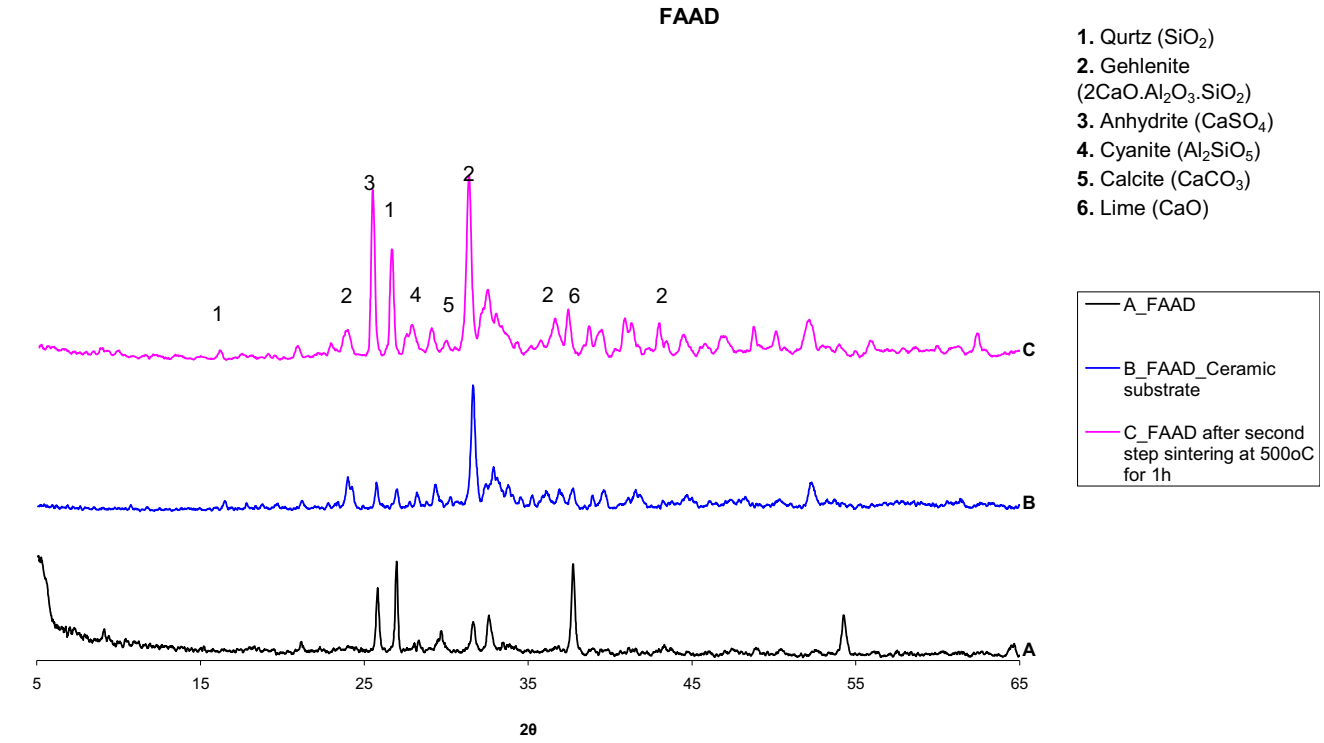

(a)

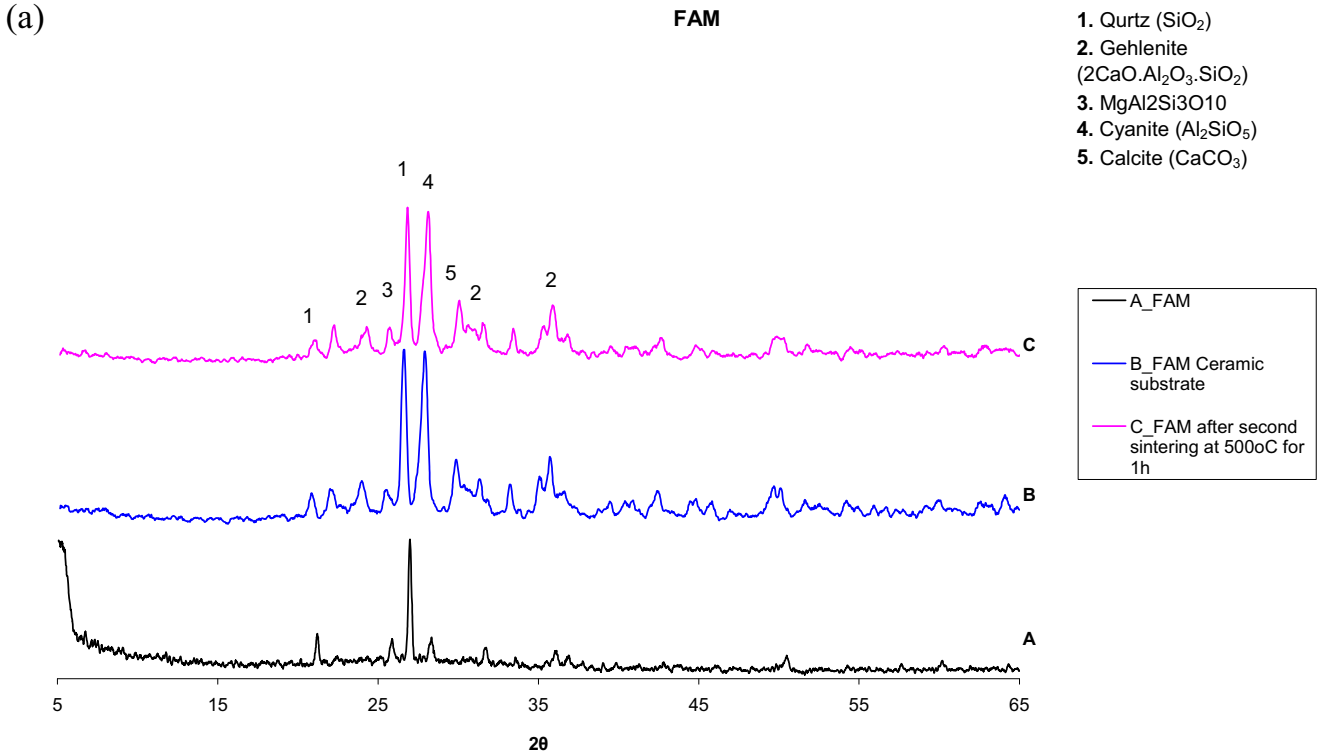

(b)

Fig. 3 XRD spectra of the ceramic substrates **a** FAAD and **b** FAM: (A) green (non-sintered), (B) after sintering at 1000 °C, and (C) after further thermal treatment of the coated substrates at 500 °C for 1 h

after the thermal treatment, gehlenite, anhydrite, and quartz are the main phases.

For FAM green specimens, quartz (SiO_2) is the predominant phase (Fig. 3b (A)), while quartz, cyanite, and gehlenite are

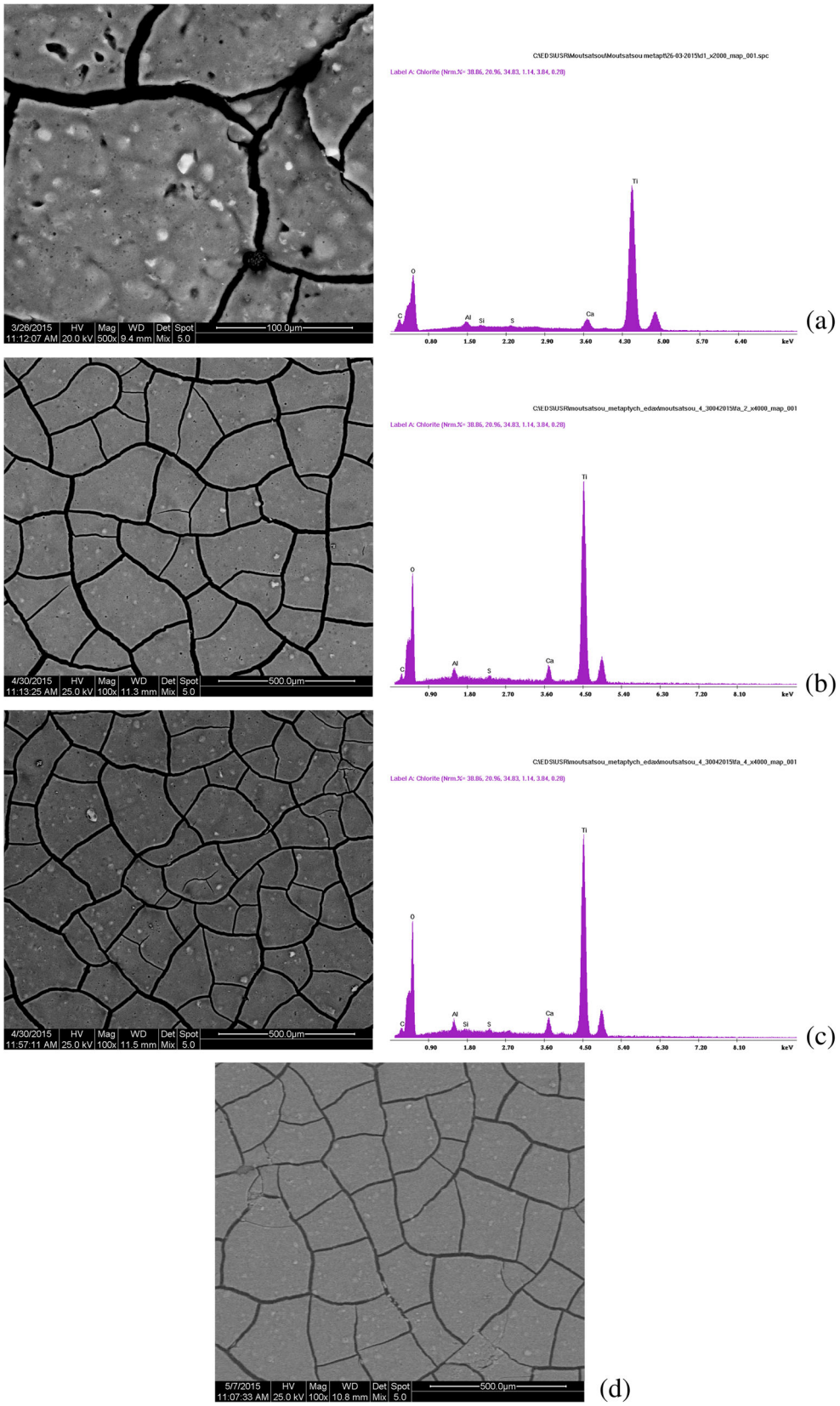

Fig. 4 SEM micrographs of the surface coating of the ceramic substrates: dried in air (**a**), and thermally treated for 1 h at 400 °C (**b**), 500 °C (**c**), and 700 °C (**d**)

detected, after sintering the specimens up to 1000 °C (Fig. 3b (B)). The same phases appear in the substrates further thermally treated after coating (Fig. 3b (C)). Therefore, it can be concluded that the mineralogical phases detected after further heating of the

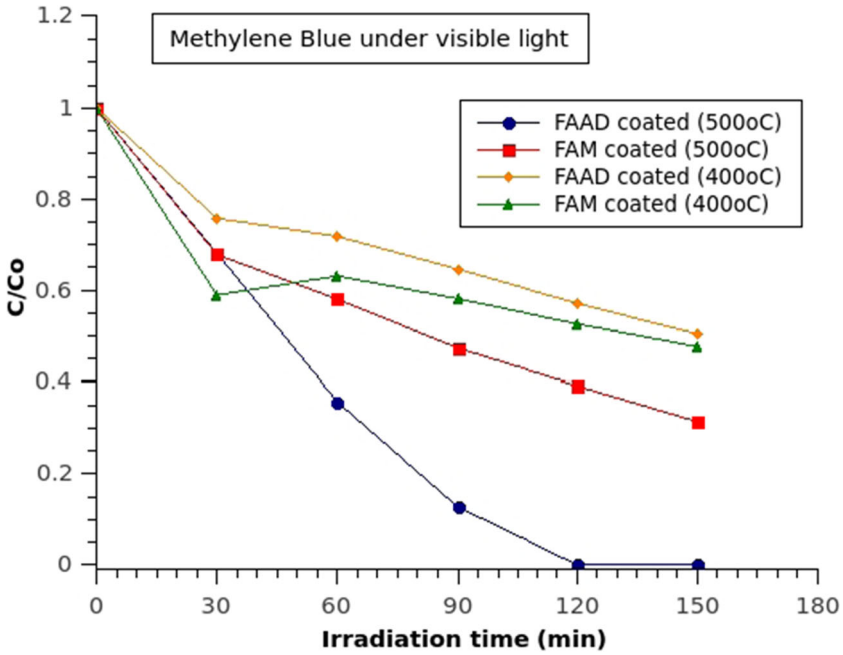

Fig. 5 Methylene blue (MB) removal under visible irradiation as a function of time

coated substrates were already generated during main sintering process and no further mineralogical change is observed.

SEM micrographs of the surface coating of the ceramic substrates after different thermal treatment conditions are given in Fig. 4. Surface coating cracks are clearly seen on the ceramic substrates due to the removal of water and degradation of the organic compounds of the slurry during heating. The surface roughness of the TiO_2-coated substrates after their thermal treatment at 500 °C was found to be 15.8 Sa (μm) for FAAD and 5.81 Sa (μm) for FAM.

The apparent density of the sintered substrates lies in the range of 1.17–1.78 g/cm^3. The Vickers microhardness for the green specimens is 230 HV and raises up to 469 HV after sintering.

Experimental results in respect of the potential of the ceramic substrates developed for adsorption of heavy metals (Cu, Pb, Cd, and Zn) show a decrease in adsorption capacity of the substrate after their coating with TiO_2 slurry, as the porous surface is rather fulfilled with TiO_2, which was verified by SEM-EDAX.

The photocatalytic activity of TiO_2-coated ceramic substrates made of FA is illustrated in Figs. 5 and 6 that show the

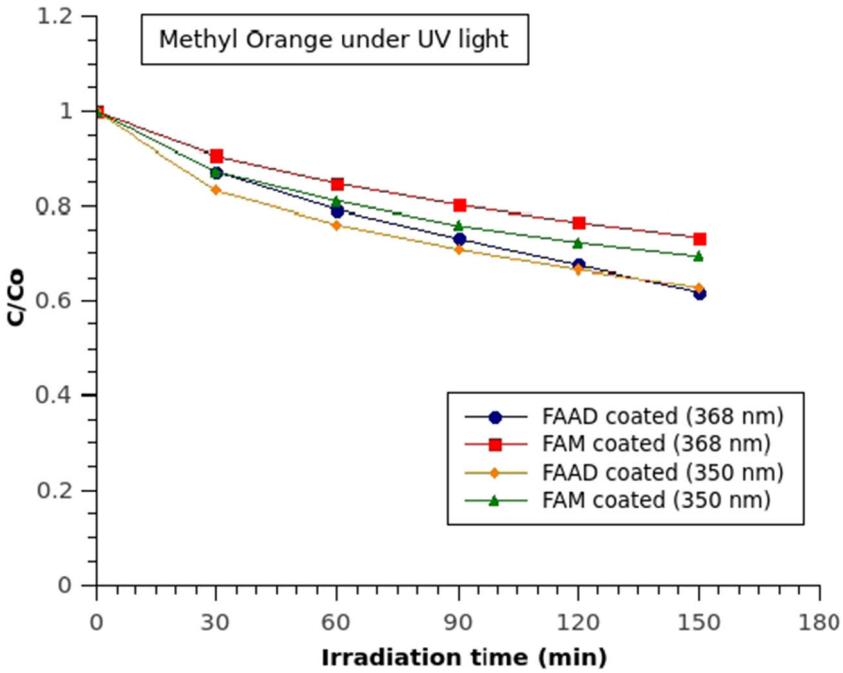

Fig. 6 Methyl orange (MO) removal under the two types of UV-A light as a function of time

decomposition kinetics for methylene blue (MB) and methyl orange (MO) respectively (dye removal in the aqueous solution as a function of irradiation time). The whole beneficial effect of the two concurrent phenomena (adsorption and photocatalysis) taking place on the total pollutant removal process is evaluated.

Concerning the experiments under visible light (Fig. 5), the decolorization of MB in the aqueous solution is very intense. Both TiO_2-coated substrates (FAAD and FAM) thermally treated at 500 °C show increased efficiency compared to those treated at 400 °C. The highest activity is exhibited by the ceramic substrates made of FAAD. Dye removal from the solution can partially be attributed to dye adsorption onto the porous and cracked coating, taking into consideration the aforementioned surface roughness results. It can, therefore, be assumed that during the experiments a combined mechanism takes place, which includes both adsorption and photodegradation.

On the other side, the removal of MO under the two types of UV-A irradiation (Fig. 6) is less pronounced than in the case of MB experiments under visible light. This finding should be correlated to other system parameters. Especially, high solution pH values encountered due to the alkaline nature of the ashes favor the adsorption of the cationic MB dye onto the substrate surface, whereas the removal of the anionic MO dye is negatively affected.

The current work mainly focused on the valorization of the lignite ashes in the elaboration and comparison of new substrates for the immobilization of the photocatalyst. Nevertheless, apart from the role of the ashes as the substrate, a major advantage is the remaining adsorption capacity of the substrate itself. In the overall pollutant decomposition process, a combined mechanism takes place, where two separate phenomena of adsorption and photodegradation participate. Therefore, the result of dye decolorization using the final activated product can be attributed to the synergistic effect between the ceramic substrates made of lignite ashes and the TiO_2, with the lignite ashes acting as the adsorptive materials and the TiO_2 providing the photocatalytic activity.

Conclusions

Effectively solidified ceramic substrates with interesting mineralogy and microstructure were produced from calcareous and siliceous lignite fly ashes.

TiO_2 films were successfully deposited onto the surface of the ceramic substrates, and the photocatalytic activity of the coated specimens appears to be remarkable, leading to the decolorization of methylene blue under visible light. Removal of methyl orange under UV irradiation is less pronounced due to the anionic nature of this dye, as the results are affected by the system pH.

It seems that ceramic substrates made of abundant calcareous lignite fly ashes provide an effective combination with TiO_2, with regard to the main goal of the current research, the degradation of organic pollutants. Due to the synergistic effect of the ceramic substrates made of lignite ashes with TiO_2, the results for dye removal appear to be encouraging for further development of photocatalytic substrates starting from industrial secondary resources, towards circular economy.

References

1. Yao, Z.T., Ji, X.S., Sarker, P.K., Tang, J.H., Ge, L.Q., Xia, M.S., Xi, Y.Q.: A comprehensive review on the application of coal fly ash. Earth Sci Rev. **141**, 105–121 (2015)
2. Karayannis, V., Spiliotis, X., Domopoulou, A., Ntampegliotis, K., Papapolymerou, G.: Optimized synthesis of construction ceramic materials using high-Ca fly ash as admixture, Revista Romana de Materiale/Romanian. J Mater. **45**(4), 358–363 (2015)
3. Kritikaki, A., Zaharaki, D., Komnitsas, K.: Valorization of industrial wastes for the production of glass-ceramics. Waste Biomass Valoriz. **7**(4), 885–898 (2016)
4. Karamberi, A., Orkopoulos, K., Moutsatsou, A.: Synthesis of glass-ceramics using glass cullet and vitrified industrial by-products. J Eur Ceram Soc. **27**(2–3), 629–636 (2007)
5. Tsimas, S., Moutsatsou-Tsima, A.: High-calcium fly ash as the fourth constituent in concrete: problems, solutions and perspectives. Cem Concr Compos. **27**(2), 231–237 (2005)
6. Karayannis, V.G., Moutsatsou, A.K., Katsika, E.L.: Synthesis of microwave-sintered ceramics from lignite fly and bottom ashes. J Ceram Process Res. **14**(1), 45–50 (2013)
7. Moutsatsou, A., Karayannis, V., Matsas, D., Katsika, E., Tsipoura, S.: "Microstructure analysis of sintered lignite combustion ashes", pp.1–9, in: A Global Road Map for Ceramic Materials and Technologies: Forecasting the Future of Ceramics, International Ceramic Federation–2nd International Congress on Ceramics, ICC (2008)
8. Young Park, J.: Assessing determinants of industrial waste reuse: the case of coal ash in the United States. Resour Conserv Recycl. **92**, 116–127 (2014)
9. Chen, W.-F., Koshy, P., Adler, L., Sorrell, C.C.: Photocatalytic activity of V-doped TiO_2 thin films for the degradation of methylene blue and rhodamine B dye solutions. J Aust Ceram Soc. **53**(2), 569–576 (2017)
10. Katsanaki, A.: Photocatalytic activity of nanostructured titanium oxide materials in standardized reactors of air pollutants, PhD Thesis, National Technical University of Athens (NTUA), Athens (2012)
11. Soutsas, K., Karayannis, V., Poulios, I., Riga, A., Ntampegliotis, K., Spiliotis, X., Papapolymerou, G.: Decolorization and degradation of reactive azo dyes via heterogeneous photocatalytic processes. Desalination. **250**(1), 345–350 (2010)
12. Lei, X., Xue, X.: Preparation, characterization and photocatalytic activity of sulfuric acid-modified titanium-bearing blast furnace slag. Trans Nonferrous Metals Soc China. **20**(12), 2294–2298 (2010)
13. Shi, J.-W., Chen, S.-H., Wang, S.-M., Wu, P., Xu, G.-H.: Favorable recycling photocatalyst TiO_2/CFA: effects of loading method on the structural property and photocatalytic activity. J Mol Catal A Chem. **303**(1–2), 141–147 (2009)
14. Adam, F., Appaturi, J.N., Thankappan, R., Nawi, M.A.M.: Silicatin nanotubes prepared from rice husk ash by sol-gel method: Characterization and its photocatalytic activity. Appl Surf Sci. **257**, 811–816 (2010)

15. Huo, P., Yan, Y., Li, S., Li, H., Huang, W.: Floating photocatalysts of fly-ash cenospheres supported AgCl/TiO_2 films with enhanced rhodamine B photodecomposition activity. Desalination. **256**, 196–200 (2010)
16. Zan, L., Fa, W., Peng, T., Gong, Z.-K.: Photocatalysis effect of nanometer TiO_2 and TiO_2-coated ceramic plate on hepatitis B virus. J Photochem Photobiol B Biol. **86**, 165–169 (2007)
17. Yu, Y.T.: Preparation of nanocrystalline TiO_2-coated coal fly ash and effect of iron oxides in coal fly ash on photocatalytic activity. Powder Technol. **146**, 154–159 (2004)
18. Arin, M., Lommens, P., Avci, N., Hopkins, S.C., De Buysser, K., Arabatzis, I.M., Fasaki, I., Poelman, D., Van Driessche, I.: Inkjet printing of photocatalytically active TiO_2 thin films from water based precursor solutions. J Eur Ceram Soc. **31**, 1067–1074 (2011)
19. Ibhadon, A.O., Greenway, G.M., Yue, Y., Falaras, P., Tsoukleris, D.: The photocatalytic activity and kinetics of the degradation of an anionic azo-dye in a UV irradiated porous titania foam. Appl Catal B Environ. **84**, 351–355 (2008)
20. Houas, A., Lachheb, H., Ksibi, M., Elaloui, E., Guillard, C., Herrmann, J.-M.: Photocatalytic degradation pathway of methylene blue in water. Appl Catal B Environ. **31**, 145–157 (2001)
21. Tsoukleris, D.S., Kontos, A.I., Aloupogiannis, P., Falaras, P.: Photocatalytic properties of screen-printed titania. Catal Today. **124**, 110–117 (2007)
22. Kontos, A.I., Kontos, A.G., Tsoukleris, D.S., Vlachos, G.D., Falaras, P.: Superhydrophilicity and photocatalytic property of nanocrystalline titania sol–gel films. Thin Solid Films. **515**, 7370–7375 (2007)